Quantitative Assessment of Ventilation-Perfusion Mismatch by Radioxenon Imaging of the Lung

Yasushi Ishii, Harumi Itoh, Teruyasu Suzuki, Yoshiharu Yonekura, Takao Mukai, and Kanji Torizuka

Kyoto University, Kyoto Japan

By the use of xenon-133 and a scintillation camera with digital data storage and processing system, a topographic relationship between ventilation distribution ($\dot{V}$) and perfusion distribution ($\dot{Q}$) was examined quantitatively in two groups of normal nonsmokers and one of older smokers, all healthy. In addition, subjects with a variety of cardiopulmonary disease were tested. The fractional regional ventilation ($\dot{V}_R$) and regional perfusion ($\dot{Q}_R$) were plotted against the $\dot{V}/\dot{Q}$ ratio on a logarithmic abscissa for the normal subjects; both were distributed log-normally with a narrow standard deviation, and were dissociated slightly from each other. However, with smoking and with increasing age, the s.d. and the dissociation became wider, suggesting an impairment of gas exchange as estimated by alveolar-atrial gas-pressure differences (A-aD), which were calculated by putting these topographic relationships into a gas-exchange program in a computer. In various cardiopulmonary diseases a good correlation was found between the estimated A-aD_{O_2} thus obtained and the actual A-aD_{O_2} derived from analysis of the blood gases.

J Nucl Med 19: 607–614, 1978

The primary function of the lung is gas exchange, which depends on the relative distribution of ventilation and perfusion in the lung. The availability of radioactive gases and external detecting probes has given rise to the complex physiological concept of ventilation-perfusion mismatch (*1*), which is signalled locally by the regional values of the ventilation/perfusion ratio (*2,3*). However, since these regional values are averaged within the field of each individual probe, the range of the mismatch is to some extent averaged, instead of showing the actual range of ventilation-perfusion inequality.

Although the advent of scintillation cameras together with digital storage and processing systems offers further possibilities for the handling of detailed information regarding these distributions within the lung (*4,5*), most of the clinical studies with such systems have merely portrayed the distributions of ventilation and perfusion independently, with regional mismatch appreciated only subjectively (*6,7*). Accordingly, a critical evaluation of their use in patient care, to assess abnormal gas exchange within a lung, has yet to be undertaken. To attain this objective, a clue to the physiological interpretation from the topographical mismatch has to be formulated.

We have developed the concept of a "functional image" to provide quantitative assessment of the relative performance of various areas of an organ as

Received July 7, 1977; revision accepted Jan. 4, 1978.

For reprints contact: Yasushi Ishii, Dept. of Radiology, Kyoto University Medical School, Sakyo-ku, Kyoto 606, Japan.

permitted by the resolution capabilities of the imaging technic (*8–10*). Whereas we have attempted to construct various types of radioxenon imaging related to regional lung function (*11*), our present concern is focused on a quantitative assessment of ventilation-perfusion mismatch from this type of pulmonary imaging. The quantitative ventilation-perfusion mismatch thus obtained evaluates the overall function of gas exchange in the lung by referring to the O_2-CO_2 diagram (*1*). This is compared with the results derived from actual blood-gas findings to see whether this type of presentation could be useful for quantitative physiological evaluation, bearing in mind the inherent constraints of the imaging procedure of a scintillation camera whose resolution and detecting capabilities are progressively restricted by source depth.

MATERIALS AND METHODS

Nine male volunteers provided a normal control group: five aged 21–25 yr and four aged 30–34; none of these had a history of tobacco smoking. In addition, there were four male volunteers, aged 35–49, who smoked more than a package of cigarettes per day. None of the foregoing had a history or symptoms suggestive of respiratory disease. The selection of these groups was intended to present the most subtle gas-exchange impairment due to smoking and aging in otherwise normal subjects. In addition, fifteen patients having a variety of cardiopulmonary diseases were randomly selected for the present investigation. There were seven patients with chronic obstructive pulmonary disease, four with mitral stenosis, three with lung cancer, and one with an atrial septal defect. All patients underwent arterial blood gas analysis within 48 hr of the radioxenon study. The arterial vs. alveolar oxygen difference ($A\text{-}aD_{O_2}$) was calculated as the difference between the mean alveolar partial pressure of oxygen (P_{AO_2}), computed from the ideal alveolar air equation, and the measured PO_2 in all patients.

Patients were examined in a sitting position. A scintillation camera with a diverging collimator viewed the whole of both lung fields from behind. Approximately 10 mCi of xenon-133 gas were administered in a slow single inspiration from the level of the functional residual capacity to the level of resting inspiration. This was achieved by inhaling 500 ml of air from a rubber bag containing the tracer gas through a narrow side tube attached to a mouthpiece. The patient then held his breath while the ventilation distribution ($\dot{V}$) was obtained by the recording camera. He next rebreathed the gas within a closed spirometer circuit for 3–4 min, the equilibrated gas distribution being considered to represent the volume distribution (V) in the lung. He continued breathing at resting tidal level until an adequate total count had been collected. With the subject seated in the same position, approximately 5 mCi of Xe-133 in solution were injected intravenously. The initial distribution in the lung then represented the perfusion distribution ($\dot{Q}$), recorded during a breath-hold with open glottis at the level of resting inspiration.

These camera images were processed by a digital computer, point by point, in a 40 × 40 word matrix (*10*). The ratio of ventilation to perfusion ($\dot{V}/\dot{Q}$) was displayed in the form of an isocontour image with ten levels, as shown in Fig. 1. Before the calculation, the functional contour of each lung was determined by cutting off a region having less than 20% of the maximum activity of the equilibrated image (V)—i.e., the lower two levels of the isocontour image were excluded as representing nonrespiratory radioactivity. The total counts in the $\dot{V}$ and $\dot{Q}$ lung fields were then equalized to provide normalization, and a smoothing program involving nine-element bounding was applied (*8,10*).

Since an actual ventilation/perfusion ratio ($\dot{V}_A/\dot{Q}_C$) cannot be known in the absence of data regarding pulmonary capillary blood flow ($\dot{Q}_C$) and alveolar ventilation ($\dot{V}_A$), we have adopted a value of 0.85 as normal for the ratio $\dot{V}_A/\dot{Q}_C$, in accord-

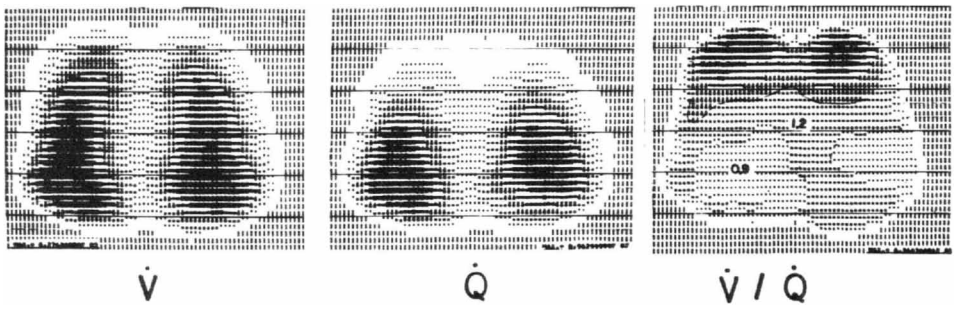

FIG. 1. Processed radioxenon imaging of pulmonary ventilation ($\dot{V}$) and perfusion ($\dot{Q}$), from which ventilation/perfusion ratio ($\dot{V}/\dot{Q}$) was constructed. Normal subject in upright position.

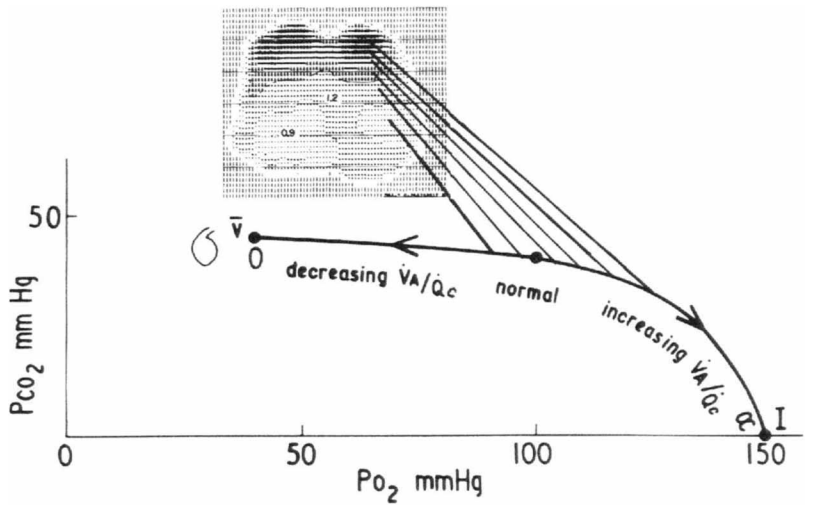

FIG. 2. Illustrating relation between $\dot{V}/\dot{Q}$ imaging and O_2-CO_2 diagram.

ance with the computer model proposed by West (*12*). This figure is believed to indicate that oxygen intake and CO_2 output lie within normal limits in the steady-state condition. Accordingly, each elemental value in the $\dot{V}/\dot{Q}$ image was multiplied by 0.85. From the data in the ventilation ($\dot{V}$) and perfusion ($\dot{Q}$) images, and the resultant regional $\dot{V}_R/\dot{Q}_C$ image, distribution functions were plotted for the three groups of normal subjects. The graphs are derived from histograms in which the horizontal scale covers the range of $\dot{V}_A/\dot{Q}_C$ from 0.2 to about 3 in ten steps, the increments being ratios rather than differences. Thus the scale is logarithmic, with the right-hand edge of each bar about 30% higher than its left-hand edge ($0.2 \times 1.3^{10} \approx 3$). The ordinate for a given bar is the fraction of the total pulmonary radioactivity ($\dot{V}$ or $\dot{Q}$ as the case may be) that lies within that bar's range. These "fractional contributions" are then plotted (as percentages)—$\dot{V}_R$ as a fraction of $\dot{V}$, and $\dot{Q}_R$ as a fraction of $\dot{Q}$.

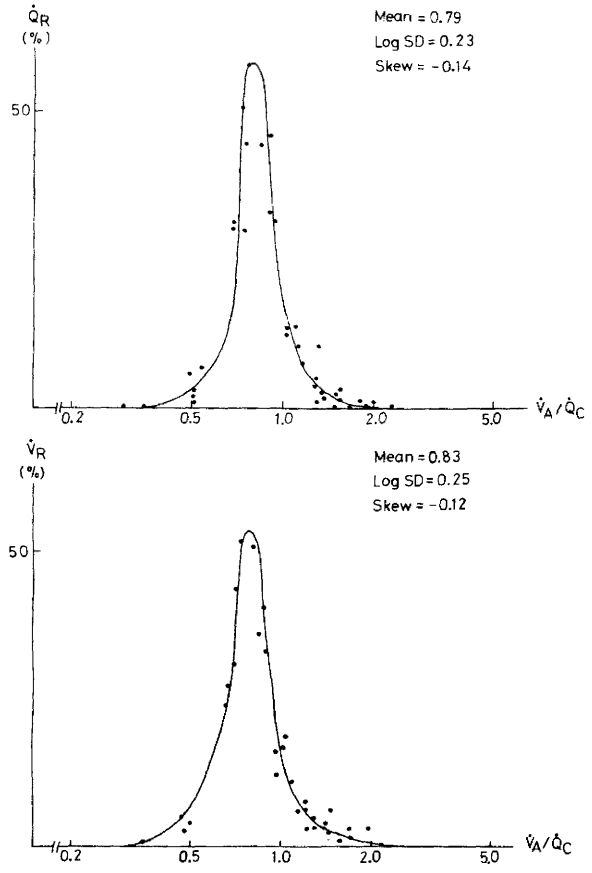

FIG. 3. Fractional distributions of ventilation ($\dot{V}_R$) and perfusion ($\dot{Q}_R$) with respect to ventilation-perfusion ratio ($\dot{V}_A/\dot{Q}_C$), with logarithmic scale, in young nonsmokers.

At any given lung region, the relations between $\dot{V}_R$ and $\dot{V}_A/\dot{Q}_C$, and between $\dot{Q}_R$ and $\dot{V}_A/\dot{Q}_C$, can be used to estimate overall gas-exchange efficiency, calculating the differences, for O_2 and CO_2, between alveolar and arterial pressures—that is, A-aD_{O_2} and A-aD_{CO_2}—by a computer (*12*) (Fig. 2).

RESULTS

Distribution of ventilation/perfusion ratio of normal lung. Processed images from a normal subject in the upright position are shown in Fig. 1. The effects of gravity on the lung (*13*) are evident in the $\dot{V}$ and $\dot{Q}$ images, and an inverted gravitational pattern (decreasing toward the base) is seen in the $\dot{V}/\dot{Q}$ image.

Total accumulative counts per frame of the original images of $\dot{V}$, V, and $\dot{Q}$ were more than 50,000, and in each element the maximum counts were over 100. The $\dot{V}/\dot{Q}$ image was constructed by a simple division of these two original images, and the s.d. percentage for the quotient, after applying the elemental bounding, was found to lie between 5 and 10%. (Counts less than 20% of maximum activity

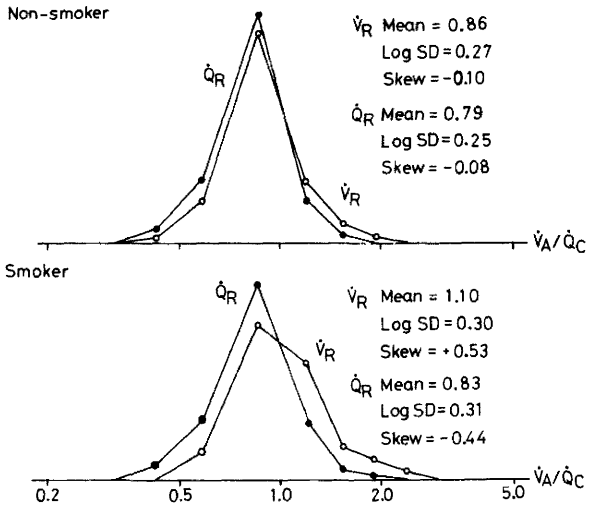

FIG. 4. Fractional distributions of $\dot{V}_R$ (circles) and $\dot{Q}_R$ (dots) with respect to $\dot{V}_R/\dot{Q}_C$ in the older (ages 30–34) nonsmokers (upper panel) and in older (ages 35–49) smokers (lower panel).

were eliminated from the V image as previously described.)

Distribution of ventilation or blood flow with respect to ventilation-perfusion ratio in normal subjects. In order to obtain a functional, quantitative interpretation for ventilation-perfusion mismatches, and thus to estimate the gas-exchange function of the lungs, we have examined our three normal groups (Figs. 3 and 4) regarding their $\dot{V}_R$-$\dot{V}_A/\dot{Q}_C$ and $\dot{Q}_R$-$\dot{V}_A/\dot{Q}_C$ relations.

As shown in Fig. 3, plots of the $\dot{Q}_R$ & $\dot{V}_R$ distributions against logarithm of $\dot{V}_A/\dot{Q}_C$ in five young nonsmokers can be fitted approximately by a log-normal distribution function with little dispersion (log s.d. for $\dot{Q}_R = 0.23$ and that for $\dot{V}_R = 0.25$) and with little skewness (third moment being -0.14 for $\dot{Q}_R$ and -0.12 for $\dot{V}_R$). Thus both distributions are virtually symmetrical along the $\dot{V}_A/\dot{Q}_C$ axis. The $\dot{V}_A/\dot{Q}_C$ ratio for the mean $\dot{Q}_R$ was 0.79, and that for the mean $\dot{V}_R$ 0.83, so that the two distributions are dissociated slightly, with that for $\dot{V}_R$ shifted toward the right.

The average statistical moments of these distribution functions for the older nonsmokers are shown in Fig. 4, upper panel. The mean for $\dot{V}_R$ was 0.86 and for $\dot{Q}_R$ 0.79; the dispersion in terms of log s.d. was 0.27 for $\dot{V}_R$ and 0.25 for $\dot{Q}_R$; and the skewness was -0.10 for $\dot{V}_R$ and -0.08 for $\dot{Q}_R$. These findings are not significantly different from those of the younger group, although they show slightly wider dissociation between the $\dot{Q}_R$ and $\dot{V}_R$ distributions and slightly higher values of the second moments. On the other hand, those of older smoker group (lower panel) revealed more dissociation between the means of these distributions (the mean being 1.10 for the $\dot{V}_R$ and 0.83 for the $\dot{Q}_R$), and wider dispersion (log s.d. for $\dot{V}_R = 0.30$ and for $\dot{Q}_R = 0.31$) than other normal groups. They also deviated towards a higher value of $\dot{V}_A/\dot{Q}_C$ for $\dot{V}_R$ and lower value for $\dot{Q}_R$, the skew being 0.53 for $\dot{V}_R$ and -0.44 for $\dot{Q}_R$.

Along with the changes of these moments in each group, the computer values of A-aD_{O_2} and A-aD_{CO_2} became numerically increased, as is seen in Table 1. The A-aD_{O_2} advanced from 6.9 mm Hg in the young nonsmokers to 14.3 in the older smokers, while the A-aD_{CO_2} increased numerically from -0.18 in the first group to -1.03 in the last.

Distribution of ventilation or blood flow with respect to ventilation-perfusion ratio in various cardiopulmonary diseases. Table 1 also gives the findings from a similar processing of the 15 patients selected for a variety of cardiopulmonary diseases. In general, the mean of these two distribution functions dissociated with wider dispersion and a high degree of skewness, depending on the nature of the disease. In order to derive the functional implications of these distribution functions, A-aD_{O_2} and A-aD_{CO_2} were

TABLE 1. MEANS OF A-aD ESTIMATED FROM BLOOD GASES AND FROM VARIOUS PARAMETERS OF DISTRIBUTION FUNCTION OF $\dot{V}_A/\dot{Q}_C$

					Distribution function of $\dot{V}_A/\dot{Q}_C$					
		Alveolar	Computer		$\dot{V}_R - \dot{V}_A/\dot{Q}_C$			$\dot{Q}_R - \dot{V}_A/\dot{Q}_C$		
		A-aD_{O_2}	A-aD_{O_2}	A-aD_{CO_2}	Mean	Log s.d.		Mean	Log s.d.	Skew
Young nonsmokers	Mean	—	6.9	−0.18	0.83	0.25	−0.12	0.79	0.23	−0.14
(n = 5)	s.d.	—	±3.9	±0.22	±0.03	±0.03	±0.07	±0.02	±0.02	±0.06
Older nonsmokers	Mean	—	9.3	−0.39	0.86	0.27	−0.10	0.79	0.25	−0.08
(n = 4)	s.d.	—	±4.5	±0.43	±0.04	±0.03	±0.09	±0.02	±0.02	±0.07
Smokers	Mean	—	14.3	−1.03	1.10	0.30	+0.53	0.83	0.31	−0.44
(n = 5)	s.d.	—	±4.6	±0.46	±0.04	±0.05	±0.31	±0.03	±0.04	±0.21
Patients	Mean	16.1	14.0	−1.11	1.02	0.44	0.00	0.80	0.38	−0.10
(n = 15)	s.d.	5.2	±7.4	±0.65	±0.13	±0.12	±0.47	±0.07	±0.11	±0.43

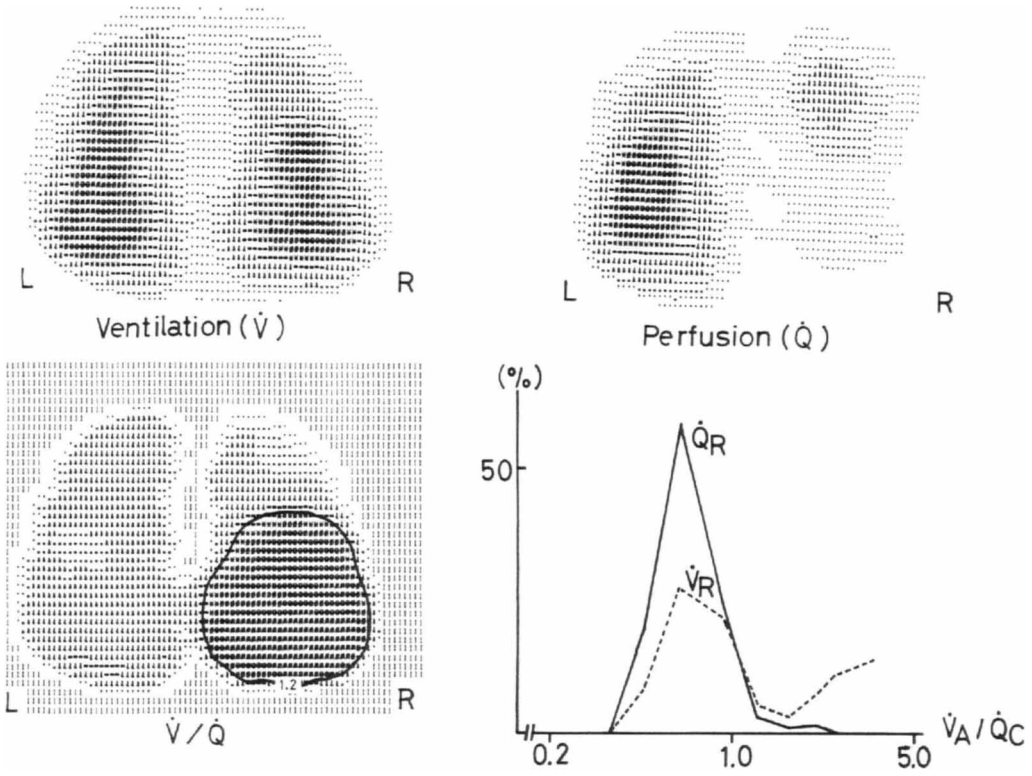

FIG. 5. Images providing $\dot{V}/\dot{Q}$, and the distributions of fractional $\dot{V}_R$ (dashed line) and $\dot{Q}_R$ (solid line) as a function of $\dot{V}_A/\dot{Q}_C$ in a patient with bronchogenic carcinoma.

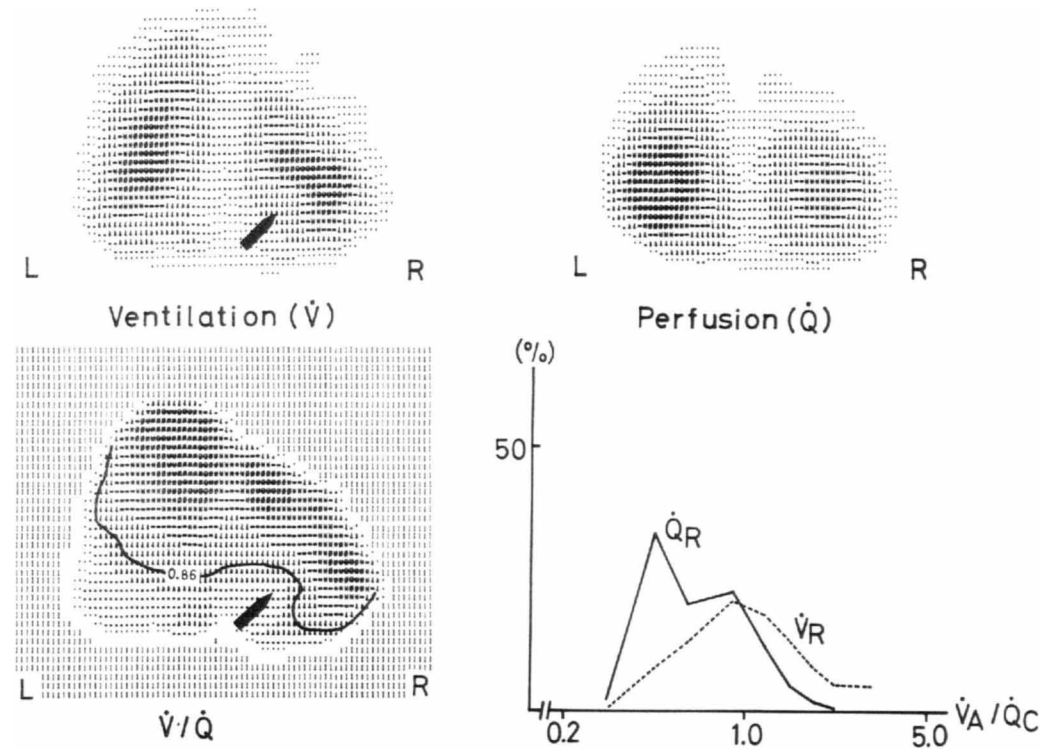

FIG. 6. Images providing $\dot{V}/\dot{Q}$, and the distributions of fractional $\dot{V}_R$ (dashed line) and $\dot{Q}_R$ (solid line) as a function of $\dot{V}_A/\dot{Q}_C$ in a patient with chronic obstructive pulmonary disease.

calculated by putting the scintigraphic data into the gas-exchange program and comparing the results with those obtained from actual blood-gas measurements.

Study of the ventilation/perfusion images suggests that ventilation-perfusion mismatches tend to fall into two main types. One presents regions with high $\dot{V}/\dot{Q}$ ratio where a considerable fraction of ventilation ($\dot{V}_R$) distributes towards the high $\dot{V}_A/\dot{Q}_C$ regions; the other presents regions with low $\dot{V}/\dot{Q}$ where a considerable fraction of perfusion ($\dot{Q}_R$) distributes towards low $\dot{V}_A/\dot{Q}_C$ regions. A case with bronchogenic carcinoma at the right intermediate bronchus illustrates the former type in the right lower lobe, as shown in Fig. 5; the A-aD_{O_2} and A-aD_{CO_2} estimated from these distributions gave 16.5 mm Hg and −1.94 mm Hg, respectively, indicating the presence of a dead-space effect with a wide carbon dioxide difference. Figure 6 illustrates the second type, a case with chronic obstructive disease of both lower lung regions; alveolar-arterial gas differences were estimated to be 29.3 mm Hg for oxygen and −0.86 mm Hg for carbon dioxide, indicating the presence of a physiological shunt effect with a wide oxygen difference.

To investigate the effect of a graded change of the distribution function on overall gas-exchange efficiency, we have listed in Table 2 the differences between the means for the $\dot{V}_R$ and $\dot{Q}_R$ distributions ($\dot{Q}_R$-$\dot{V}_R$) as a measure of the dissociation between these two. We also list the logarithmic s.d. of the $\dot{Q}_R$ distribution (log s.d. of $\dot{Q}_R$) as a plausible index for the presence of a physiological shunt effect (*14*). These were compared with ideal alveolar A-aD_{O_2}, which showed a probable positive correlation with $\dot{Q}_R$-$\dot{V}_R$ ($r = 0.401$, $p < 0.25$) and with log s.d. of $\dot{Q}_R$ ($r = 0.443$, $p < 0.1$). This indicates that the distributions themselves might provide a rough index for the evaluation of overall gas exchange. However, as shown in Table 2, a significant correlation ($r = 0.924$, $p < 0.001$) was found between A-aD_{O_2}, as calculated from the topographical relationship, and that found by actual blood-gas measurements (Fig. 7). It appears, therefore, that the scintigraphic type of pulmonary study may provide a good functional resolution, in quantitative terms for a ventilation-perfusion mismatch.

TABLE 2. CORRELATION COEFFICIENTS BETWEEN PARAMETERS OF DISTRIBUTION FUNCTION OF $\dot{V}_A/\dot{Q}_C$ AND IDEAL ALVEOLAR A-aD_{O_2}

	Computer	Distribution Function of $\dot{V}_A/\dot{Q}_C$	
	A-aD_{O_2}	Log s.d. of $\dot{Q}_R$	$\dot{Q}_R - \dot{V}_R$
r	0.924*	0.443†	0.401‡

* $p < 0.001$; see Fig. 7.
† $p < 0.1$.
‡ $p < 0.25$.

DISCUSSION

The introduction of new radiographic technics such as computerized tomography will substantially alter the types of diagnostic study that we do in our nuclear medicine laboratories. A single imaging study will have to be replaced with radiotracer procedures that give functional information on each organ system. However, since such functional visualization represents merely the relative contribution of some portion of an organ to its overall functional integrity, it must be interpreted, if possible, in terms of desired physiological quantities. For example, since different ventilation/perfusion ratios are known to define various combinations of partial pressures of oxygen, carbon dioxide, and nitrogen (*1*), and thus to indicate different inputs and outputs of these gases at every functional unit of the lung, it is quite relevant for this topographical unevenness to be interpreted as an index of the gas-exchange function of the lung. Although poor resolution in a single projection of the present method may limit sophisticated analysis, this type of approach seems worth trying.

While measurements using radioactive gases with external detecting probes have demonstrated the ventilation/perfusion unevenness topographically, most of studies (*15,16*) have failed to correlate well with

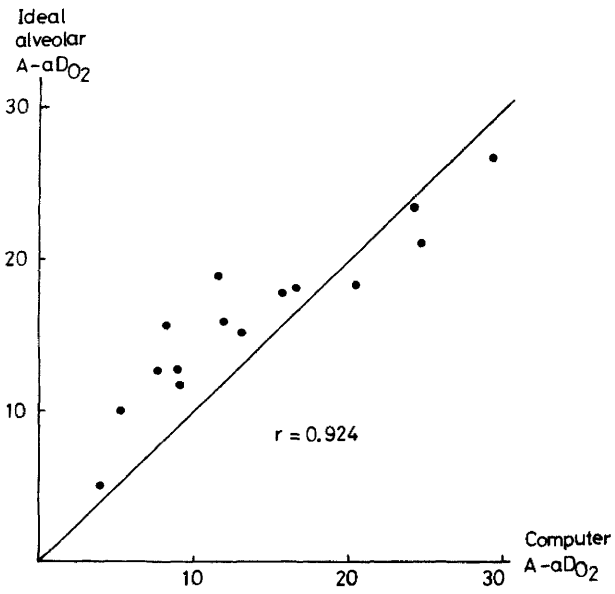

FIG. 7. Correlation between A-D_{O_2} calculated from the pulmonary imaging (abscissa) and from actual blood-gas values (ordinate).

overall impairment of lung function, indicating that several combinations of external detecting probes are not likely to resolve adequately the regional distribution of the ventilation/perfusion mismatch. Using six single probes over each side of the chest, Dawson et al. (*17*) assessed A-aD_{O_2} based on the regional ventilation/perfusion mismatch. Their calculation used almost the same procedures as ours here, referring to the O_2-CO_2 diagram, and they found a better—though not statistically significant—correlation between the estimated and actual values of A-aD_{O_2}. Although the nonhomogeneity of ventilation/perfusion ratio between large lung fields tended to be somewhat greater when overall gas exchange was more severely impaired, they concluded that most of the ventilation/perfusion unevenness was between lung units too small to be detected with large single probes. Our method, with its more detailed topographical information from a 40 × 40 matrix, does provide reasonable results and the computer system completes the tedious analysis with ease within several minutes.

To provide accurate definition of the quantitative ventilation or perfusion distribution with respect to the ventilation/perfusion ratio, Wagner et al. proposed a new analytical method to derive virtually continuous distributions of ventilation/perfusion based on the steady-state elimination of six nonradioactive gases having different solubilities (*14*). Although accurate and reliable, this method does not seem to be practical or feasible for routine clinical examinations. In this respect, a noninvasive radioactive gas method may be more useful. In comparing their results with ours, we found a fairly good correlation. Both approaches are based on virtually a log-normal distribution function with little dispersion, and reveal slight dissociation between the ventilation and perfusion distributions with higher ventilation/perfusion ratios, in young normal subjects. With both methods, the dispersions as well as dissociations of these distribution functions become wider with smoking and aging, indicating an increasing tendency for overall ventilation-perfusion mismatch, with understandable loss of gas-exchange efficiency in the lungs. However, the nonradioactive method suggests that our method is still likely to underestimate the ventilation/perfusion mismatch, since the values for the dispersion of these distribution functions, according to their method, were slightly broader than in ours (their mean log s.d. was 0.43 for the ventilation and 0.35 for perfusion in normal subjects). In spite of this probable underestimate, the demonstration of excellent correlation between estimated and measured A-aD_{O_2} supports the present approach as at least a semiquantitative means for assessment of gas-exchange function in a diseased lung, since comparable data by other nonradioactive methods are not available at present.

Our ventilation and perfusion measurements were made by a single administration during breath holding in a static state, and these are known to vary with various physiological conditions such as lung volume and inspiratory flow rate. For this reason, other investigators prefer a steady-state or dynamic measurement at resting tidal breathing (*18,19*). However, since the ventilation distribution, in the dynamic method, is calculated by the rate of elimination of a radioactive gas from the initial perfusion distribution, it is liable to be dominated by the perfusion distribution as well as by background contributions from nonpulmonary tissues. Moreover, the statistical reliability of this type of image construction is decreased by further processing (*10*). Accordingly, we chose the static measurement, which favors the collection of many counts at once, and with less background contamination.

With our present instrumentation, the most serious problem facing the quantitative assessment of ventilation-perfusion mismatch must be the deterioration of detector performance with depth. If the regional impairment of lung function follows mainly the segmental arrangement of the bronchovascular tree, the recording of lateral views might differentiate the segmental units better than the usual posterolateral views. However, in order to obtain, with good resolution, quantitative three-dimensional distributions of a radiotracer within the lung—surely a valuable goal—new instrumentation such as the positron system for transaxial reconstruction tomography should be applied (*20*). With this new device an analytical approach, as presented here, would become more useful and pertinent.

APPENDIX

$\dot{V}$ = image of ventilation distribution in the lung after a single inhalation of Xe-133.

V = image of volume distribution in the lung after rebreathing Xe-133 in a closed circuit.

$\dot{Q}$ = image of perfusion distribution in the lung after i.v. injection of Xe-133.

$\dot{V}/\dot{Q}$ = image of ventilation/perfusion ratio by point-by-point division of normalized image of $\dot{V}$ by $\dot{Q}$.

A-aD = difference between an alveolar gas pressure and its tension in arterial blood.

A-aD_{O_2} = difference between alveolar oxygen

pressure and its tension in arterial blood (mm Hg).

$A\text{-}aD_{CO_2}$ = difference between alveolar carbon dioxide pressure and its tension in arterial blood (mm Hg).

$\dot{V}/_A\dot{Q}_C$ = ratio of alveolar ventilation to pulmonary capillary blood flow, which is calculated by multiplying $\dot{V}/\dot{Q}$ by 0.85 according to the gas-exchange model proposed by West (*12*).

$\dot{V}_R$ = fractional value of regional ventilation in $\dot{V}$ image, corresponding with a specified range of $\dot{V}_A/\dot{Q}_C$.

$\dot{Q}_R$ = fractional value of regional perfusion, corresponding with a specified range of $\dot{V}_A/\dot{Q}_C$.

$\dot{Q}_R$ = mean of distribution function of $\dot{Q}_R$ plotted against a logarithmic scale of $\dot{V}_R/\dot{Q}_R$ ratio.

$\dot{Q}_R\text{-}\dot{V}_R$ = difference between $\dot{Q}_R$ and $\dot{V}_R$.

$\dot{Q}_R\text{-}\dot{V}_A/\dot{Q}_C$ = fractional distribution of perfusion for perfusion and ventilation-perfusion ratio.

$\dot{V}_R\text{-}\dot{V}_A/\dot{Q}_C$ = fractional distribution of ventilation for perfusion and ventilation-perfusion ratio.

ACKNOWLEDGMENT

This work was supported in part by a grant from Japan Tobacco & Salt Public Corporation.

REFERENCES

1. RAHN H, FAHRI LE: Ventilation-perfusion and gas exchange—The V/Q concept. In *Handbook of Physiology*, American Physiological Society, Washington, DC, 1964, pp 735–766

2. BALL WC, STEWART PB, NEWSHAM LGS, et al: Regional pulmonary function studied with 133-Xe. *J Clin Invest* 41: 519–531, 1962

3. WEST JB, DOLLRY CT: Distribution of blood flow and ventilation-perfusion ratio in the lung, measured with radioactive CO_2. *J Appl Physiol* 15: 405–410, 1960

4. NEWHOUSE MT, WRIGHT FJ, INGHAM GK, et al: Use of scintillation camera and 135-xenon for study of topographic pulmonary function. *Resp Physiol* 4: 141–153, 1968

5. LOKEN MK, MEDINA JR, LILLEHEI JP, et al: Regional pulmonary function evaluation using xenon-133, a scintillation camera and computer. *Radiology* 93: 1261–1266, 1969

6. MEDINA JR, LILLHEI JP, LOKEN MK, et al: Use of scintillation anger camera and xenon (Xe^{133}) in the study of chronic obstructive lung disease. *JAMA* 208: 985–991, 1969

7. DENARDO GL, GOODWIN DA, RAVASINI R, et al: The ventilatory lung scan in the diagnosis of pulmonary embolism. *New Engl J Med* 282: 1334–1336, 1970

8. MACINTYRE WJ, INKLEY SR, ROTH E, et al: Spatial recording of disappearance constants of xenon-133 washout from the lung. *J Lab Clin Med* 76: 701–712, 1970

9. TORIZUKA K, HAMAMOTO K, MORITA R, et al: Regional cerebral blood flow measurement with xenon-133 and the scinticamera. *Amer J Roentgenol Radium Ther Nucl Med* 112: 691–700, 1971

10. ISHII Y, KAWAMURA J, MUKAI T, et al: Functional imaging of intrarenal blood flow using scintillation camera and computer. *J Nucl Med* 16: 899–907, 1975

11. ISHII Y, MUKAI T, NOMURA S, et al: Comparative studies between ventilation and perfusion distribution in lung. *J Nucl Med* 14: 411, 1973

12. WEST JB: Ventilation-perfusion inequality and overall gas exchange in computer models of the lung. *Resp Physiol* 7: 88–110, 1969

13. WEST JB: Regional difference in gas exchange in the lung of erect man. *J Appl Physiol* 17: 893–898, 1962

14. WAGNER PD, LARAVUSO RB, UHL RR, et al: Continuous distributions of ventilation-perfusion ratios in normal subjects breathing air and 100% O_2. *J Clin Invest* 54: 54–68, 1974

15. PAIN MCF, GLAZIER JB, SIMON H, et al: Regional and overall inequality of ventilation and blood flow in patient with chronic air flow obstruction. *Thorax* 22: 453–461, 1967

16. ANTHONISEN NR, BASS H, ORIOL A, et al: Regional lung function in patients with chronic bronchitis. *Clin Sci* 35: 495–511, 1968

17. DAWSON A, ROCAMORA JM: Regional lung function and overall gas exchange in chronic obstructive lung disease: The effect of intermittent positive pressure breathing with isoproterenol. *Am Rev Resp Dis* 109: 338–344, 1974

18. ANTHONISEN NR, DOLOVICH MB, BATES DV: Steady state measurement of regional ventilation to perfusion ratio in normal man. *J Clin Invest* 45: 1349–1356, 1966

19. INKLEY SR, MACINTYRE WJ: Dynamic measurement of ventilation-perfusion with xenon-133 at resting lung volumes. *Amer Rev Respir Dis* 107: 429–441, 1973

20. TER-POGOSSIAN MM, PHELPS ME, HOFFMAN EJ, et al: A positron-emission transaxial tomograph for nuclear imaging (PETT). *Radiology* 114: 89–98, 1975